International Journal of Engineering Inventions
e-ISSN: 2278-7461, p-ISSN: 2319-6491
Volume 12, Issue 1 [January. 2023] PP: 115-120

A design-based Analysis of the Overload Capacity of the Three Phase Induction Motor.

Omogbai Nelson Oyakhilomen; Ezechukwu Oseloka Augustus.
Electrical Engineering Dept., Faculty of Engineering, Nnamdi Azikiwe University, Awka, Anambra state, Nigeria.
Corresponding Author: Omogbai, O.N.(nellsyn@yahoo.com.)

ABSTRACT: *This paper presents from the rotor bar design perspective, a salient precaution in the process of boosting the capacity for short time overload of a 3ph squirrel cage induction motor (SCIM). Two SCIM's were run in a Matlab environment for this purpose and appropriate design actions were effected on the geometry of the rotor bar transverse section to vary the breakdown torque (T_{max}), while monitoring the overload capacity. Results appear to show that shoring up the magnitude of T_{max} does not always translate into better overload capacity (OC) for the machine. The study tends to show that a good design move could be for the designer to keep an eye on the respective margins of change in both the T_{max} and the full load torque (T_{FL}), as appropriate modifications are made to the rotor and/or stator design, until the objective is achieved.*

Date of Submission: 01-08-2023 Date of acceptance: 08-01-2023

NOMENCLATURE

Symbol	Description	Unit
T_{max}	Breakdown torque	*N.m*
T_{FL}	Full load torque	*N.m*
OC	Short time overload capacity	*ohms*
R_2	Rotor Resistance	*Ohms*
X_2	Rotor Leakage Reactance	*Ohms*
R_1	Stator Coil Resistance	*Ohms*
X_1	Stator Coil Leakage Reactance	*Ohms*
X_m	Magnetizing Reactance	*Ohms*
R_c	Core Loss Resistance	*Ohms*
p.u	Per unit	*ohms*

NOITCUDORTNI

Itcould be argued that the squirrel-cage induction motor (SCIM) is the most adopted electrical machine for electrical drives being characterized by simple and robust construction, reduced maintenance requirements, technology maturity, low costs, etc. [1]. Any section of the electric drive, of which the SCIM is a part, could be designed/optimized to provide effective control of the speed-torque characteristics of the induction motor. Studies have shown that to improve the performance of a SCIM, several design variables may have to be modified; one of such adjustments being the optimization of the stator and rotor geometries [2].Designing the shape of the rotor bar cross section has a significant impact on the overall performance of the machine.

Also, in [1] as well as in [3], emphasis abound of the fact that for a three phase SCIM, rotor bar shape optimization is frequently used to achieve certain working parameters or characteristics. It is an established fact that the T_{max} is inversely proportional to the equivalent leakage inductance and is independent of rotor equivalent resistance. In [4] as well as in [5] literature support exists for the fact that the rotor slip which seems to be in charge of torque production at the linear region of SCIM operation is in turn influenced by the rotor bar resistance R_2 and weakly by the rotor leakage reactance X_2. Further, R_2 in turn is approximately equal to the inverse of the rotor bar cross-sectional area A (neglecting end-ring resistance) [6].

The authors of [1], [2] and [7] in their research discovered that by modifying the shape of the rotor bar, while keeping a constant bar area (to guarantee an acceptable power output level), various performance criteria of the SCIM could be optimized, including the T_{max}. They tried to alter the width of the bar at certain points along the bar depth by implementing some tapering (narrowing) effect on the rotor bar; carrying out actions like elongating. obliquing, stepping, constricting or kinking a portion of the transverse section. In [7] emphasis was made that the breakdown torque increased when changing the deep rectangular shape bars to the optimal stepped shape bars, with the same cross-sectional area. Note that by these shape tapering modifications there is also a resultant change in the position of the centroid of the bar area. These actions were observed to significantly affect the level of magnetic leakage around the rotor slot and ultimately, the T_{max} . The centroid as fig 1 illustrates, being the center of mass or geometric center of the rotor bar.

Overload in a three phase SCIM is not uncommon during operation due to conditions of excessive load torque, undervoltage, high friction etc. Overload operation should be for only short periods of time and very low duty cycles to prevent overheating [8].

A large breakdown torque is usually desirable either for high transient torque reserve or for widening the constant power speed range in variable frequency driven SCIMs [9], The capacity for short time overload is usually estimated as the margin between the magnitudes of the full load torque and the breakdown torque and may be approximated as the ratio of T_{max} to T_{FL}. The upper limit to torque production of the SCIM being determined by the leakage reactance [10].

EXPERIMENTAL SETUP

The experiment issuch that requires the automatic simulation of a three-phase SCIM with the geometric parameters of the rotor bar section varied by small incremental steps so that the expected torque responses could be captured.First, at a frequency of 50Hz and 400V L-L, a 100HP three-phase SCIM (M1) was run in Matlab.Second, and in line with the studies in [1], [2] and [7]; all variables of the SCIM were kept constant while altering only the geometric parameters of the rotor bar cross section such as the angle of taper (T) to introduce some narrowing effect; and the centroid (C) to alter the spatial coordinates of the bar section with respect to the airgap; in the same process the cross-sectional area A, changes accordingly. The OC responses duly estimated as the ratio betweenmaximum and full-load torque responses, were recorded against the corresponding varied geometric parameters at each instance of variation, as far as the design constraints were not violated.These modifications are moves to influence both T_{max} ,T_{FL}, and ultimately the OC. All of the foregoing procedure were repeated with a SCIM rated 75HP (M2) housing rotor bars of completely different design, so as to verify if the observed results are specific to a given machine design or generic within the family of the three-phase SCIMs; and to some extent give some result validation when both machines give agreeable results. The specifications of the machines are given in table 1:

Table 1: Experimental SCIM specifications.

Parameters	M1	M2
Number of poles (p)	8	6
Number of rotor slots (Sr)	55	55
Number of stator slots (Ss)	72	72
Conductors per slot (Cs)	4	4
Full load efficiency (EffR) %	91.12268376	91.0128091
Full load current (I1R) Amps	137.6654083	104.0402237
Full load power factor (PFR)	0.858292383	0.85131468
Full load speed (nmR) rpm	738.5338567	988.106205
Full load torque (TTdR) N.m	972.3504996	545.2107288
Starting Torque (Tst) N.m	1211.62116	1033.85206
Maximum Torque (Tmax) N.m	3368.962837	2406.639801
Starting Current (Ist) Amps	890.6527739	875.9259286
Bar current (Ib) Amps	604.1870846	442.4420793
End ring current (Ie) Amps	1322.191215	1290.975472
Voltage L-L (V) volts	400	400
X1 (ohms)	0.119190885	0.109421793
X2pr (ohms)	0.132792566	0.136917382
Xm (ohms)	3.939174055	4.741771839
R1 (ohms)	0.035604393	0.055371997
R2pr (ohms)	0.042764132	0.049826583
Rc (ohms)	110.5079781	157.5086264

The geometry of the rotor bar cross sections of the respective machines are also given in fig 1.

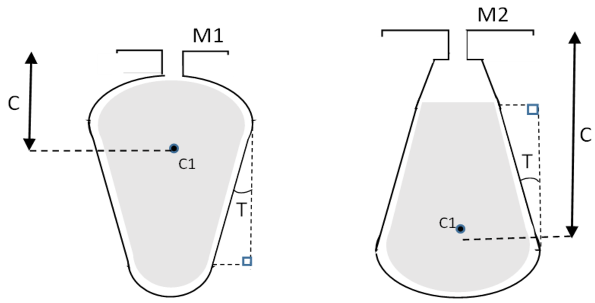

Fig 1: Rotor slot/bar geometry of the experimental machines.

RESULTS AND DISCUSSION

Table 2: Variation of bar geometry with the capacity for overload

M1							M2					
Angle of bar taper T (Degrees)	**Radial depth of the centroid of bar section C (mm)**	**Rotor bar cross-sectional area A (sq.mm)**	**Low slip R2 (ohms)**	**Low slip X2 (ohms)**	**Tmax/Tfl**		**Angle of bar taper T (Degrees)**	**Radial depth of the centroid of bar section C (mm)**	**Rotor bar cross-sectional area A (sq.mm)**	**Low slip R2 (ohms)**	**Low slip X2 (ohms)**	**Tmax/Tfl**
9.869465	12.15599	222.593972	0.035567	0.0020418	3.469446		3.4473974	12.42948	146.2207	0.049824	0.001628	4.414146
9.8415074	12.10313	220.5981289	0.035893	0.0020413	3.46935		3.5485011	12.38085	145.0788	0.050222	0.00163	4.412015
9.813228	12.05025	218.6113214	0.036225	0.0020407	3.468997		3.6511728	12.33215	143.9408	0.050625	0.001631	4.410152
9.7846213	11.99736	216.6335495	0.03656	0.0020401	3.468383		3.7554489	12.28337	142.8068	0.051033	0.001632	4.408075
9.7556815	11.94446	214.664813	0.036901	0.0020396	3.468395		3.8613663	12.23453	141.6768	0.051446	0.001633	4.40585
9.7264028	11.89154	212.7051121	0.037246	0.002039	3.46824		3.9689635	12.18561	140.5508	0.051865	0.001634	4.40402
9.6967793	11.83861	210.7544467	0.037596	0.0020384	3.467817		4.07828	12.13663	139.4287	0.052288	0.001635	4.40197
9.6668047	11.78566	208.8128169	0.037951	0.0020378	3.467458		4.1893565	12.08757	138.3106	0.052717	0.001636	4.399711
9.636473	11.7327	206.8802226	0.03831	0.0020372	3.467461		4.3022349	12.03843	137.1965	0.053152	0.001637	4.397889
9.6057776	11.67972	204.9566638	0.038675	0.0020367	3.467189		4.4169585	11.98923	136.0864	0.053592	0.001638	4.395842
9.574712	11.62672	203.0421406	0.039045	0.0020361	3.466641		4.5335722	11.93995	134.9802	0.054037	0.001639	4.393598
9.5432694	11.57371	201.1366529	0.039421	0.0020355	3.466722		4.6521219	11.89059	133.878	0.054488	0.00164	4.39176
9.5114431	11.52069	199.2402007	0.039801	0.0020349	3.466562		4.7726552	11.84116	132.7798	0.054946	0.001641	4.38969
9.4792259	11.46765	197.3527841	0.040187	0.0020342	3.466118		4.8952213	11.79165	131.6855	0.055409	0.001642	4.387507
9.4466107	11.41459	195.474403	0.040579	0.0020336	3.466064		5.0198708	11.74206	130.5953	0.055878	0.001644	4.385626
9.4135899	11.36151	193.6050574	0.040976	0.002033	3.465976		5.1466562	11.69239	129.509	0.056353	0.001645	4.383507
9.3801561	11.30842	191.7447474	0.04138	0.0020324	3.465595		5.2756315	11.64265	128.4266	0.056835	0.001646	4.381421
9.3463014	11.25531	189.8934729	0.041789	0.0020318	3.465507		5.4068526	11.59282	127.3483	0.057323	0.001647	4.379472
9.3120179	11.20218	188.0512339	0.042204	0.0020311	3.465451		5.5403772	11.54292	126.2739	0.057817	0.001648	4.377191
9.2772974	11.14903	186.2180305	0.042625	0.0020305	3.465044		5.6762652	11.49293	125.2035	0.058318	0.001649	4.374817
9.2667948	11.13309	185.6698314	0.042753	0.0020303	3.464762		5.7451146	11.46791	124.6698	0.058572	0.00165	4.373618

The designer may decide to effect a change in X_2 by modifying various geometries of the bar cross section such as the top width, radial depth, taper angle or narrowness, the distance of the bar from the airgap etc. but in this study, the latter two methods were used; hence the need to modify the angle of taper T and the radial depth of the centroid C respectively, as illustrated in fig 1 Recall that a decrease in T is likely to reduce the cross-slot flux (higher reluctance created in the cross slot path) and/or encourage the flow of more current (from the increase in area) that could saturate the leakage flux path at high slip [16]. Similar results may be got from the improvement of the magnetic coupling coefficient [11] by reducing the centroid depth C; since [12] opines that the information about the spatial coordinates of an object with homogeneous mass may be borne by its centroid. All these bar design actions tend to lead to the reduction in X_2, and then an increase in the T_{max} [13].

Meanwhile, and as previously alluded to, these geometric modifications invariably result in a change in the bar cross-sectional area A; which has been proven to be very influential over the torque developed at low slip. Also, since the significance of X_2 increases at low slip during overloads and prior to leakage path saturation [14], the modification in T for instance should be done carefully so as not to result in an unintended change e.g. offsetting an already optimal magnetic coupling depth of the bar centroid.

If these dynamics ultimately brings about an increase in both T_{max} and T_{FL}, then the change in the overload capacity will then depend on which of theseaffected torques actually changed by a greater or lesser margin in response to the change made to the bar geometry. For instance, fig 2 displays the trendlines and gradients for T_{max} and T_{FL} for both machines. It may be observed for M1 that both torques tend to increase together, but the gradient (coefficient of x in the linear equation) tells which increases at a higher rate - T_{FL} (having a gradient of about 0.0001 p.u). This seems to imply as illustrated that the overload capacity decreases as both torques are increasing, being governed by the magnitude of T_{FL}. On the other hand, M2 looks a bit different in fig 3. While T_{max} decreases, T_{FL} tends to increase, and the gradients tell us that T_{max} seems to be decreasing at a relatively greater rate (having a gradient of about 0.0001 p.u). This seems to imply as illustrated that the overload capacity will be controlled by the T_{max} .

This appears noteworthy for the designers, since they need to keep their eyes on the margins of change of both T_{max} and T_{FL} as they try to design T and/or C (or any other geometric parameter) for overload capacity optimization. [14] gave support that overload capacity does not always increase with T_{max} .

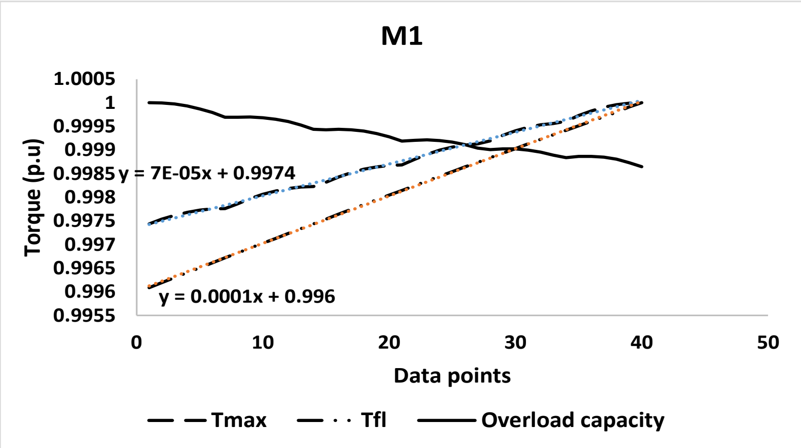

Fig 2: Changes in T_{FL} controls the overload capacity.

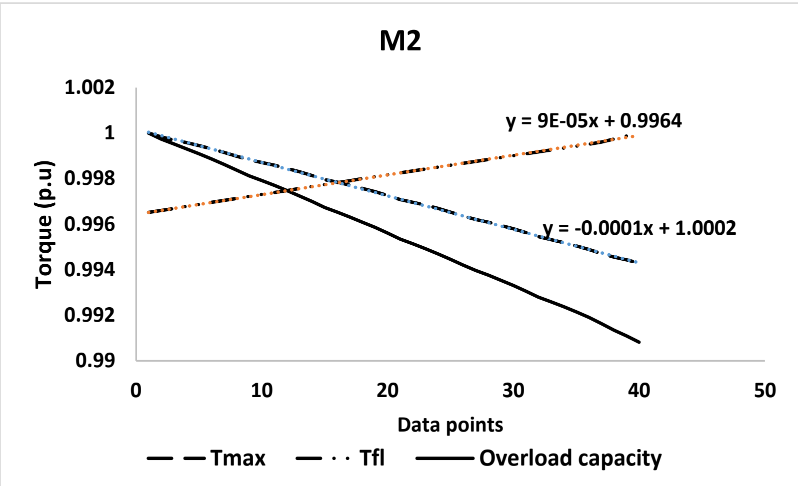

Fig 3: Changes in T_{max} controls the overload capacity.

Also, [13] clarified that the higher the slip for a given load torque, the more the machine losses. Maximum efficiency is usually at or below full load, otherwise, the copper losses rises faster than the output power [10].Taking a further look at the figures, it may also be observed that it does appear that as the magnitude of slip associated with a given load torque increases, (perhaps due to a design modification on the rotor assembly to shore up R_2) the more is the magnitude of source current consumed for normal operation (fig 4) and even for short time overload. These kinds of designs that stretches out the torque-slip curve tends to lower the operating efficiency [15]. Therefore, as the T_{max} -influencing geometric parameters are being modified for good performance in the high slip region, the design parameter A, being dominant in the low slip region, should be modified without sacrificing efficiency. Fig 5 seem to show that the operating efficiency increases with the area of the bar section, as also supported by [16] & [17].

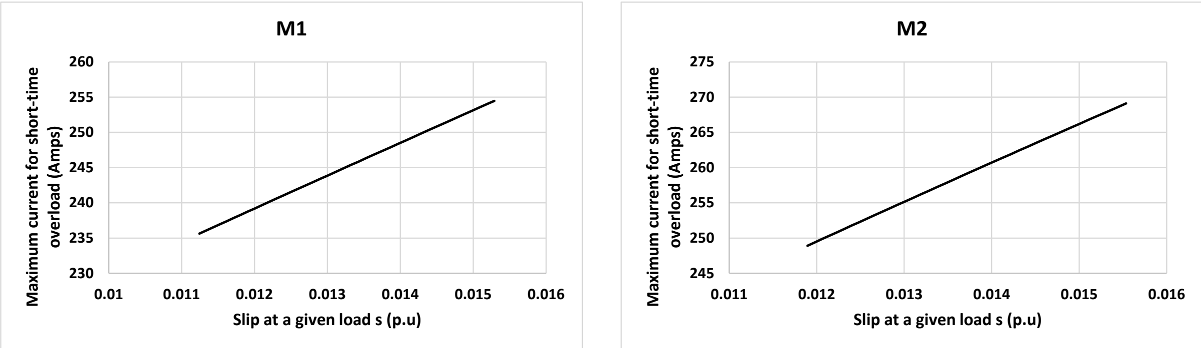

Fig 4: Slip and the overload limit.

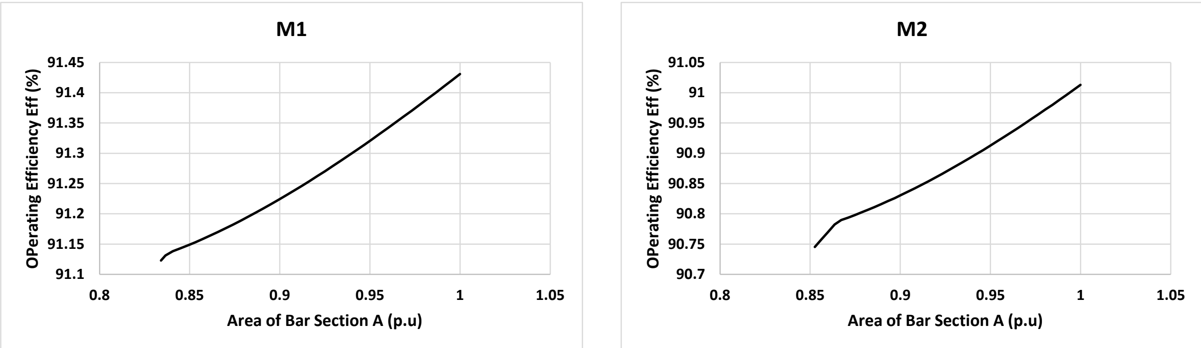

Fig 5:Bar area vs Efficiency.

CONCLUSION

More light seems to have been shed on the concept of short time overload capacity in that; designing to shore up T_{max} , does not automatically improve the transient overload capacity of the SCIM except when the percentage increase in T_{max} exceeds that obtained for T_{FL}. A surer design move appears to be for the designer to keep an eye on the respective margins of change in both T_{max} and T_{FL}, as appropriate modifications are being made to the rotor and/or stator design, until the objective is achieved. It seems evident also that in a bid to uphold the objective of high capacity for short time overload, the cross-sectional area of the rotor bar must remain as large as practicable, so that a low value of R_2 (and thus lower slip for agiven torque) will ensure that overload occurs at a relatively lower ampere cost.

REFERENCES

[1]. Turcanu, O. A., Tudorache, T. and Fireteanu, T. (2006). Influence of squirrel-cage bar cross-section geometry on induction motor performances. A paper presented at the International Symposium on Power Electronics, Electrical Drives, Automation and Motion.in Sicily, Italy. held at Taormina on the 23 – 26 May, 2006.
[2]. Di Nardo, M., Marfoli, A., Degano, M., Gerada, C. and Chen, W. (2020). Rotor design optimization of squirrel cage induction motor - part II: results discussion. IEEE. 1 – 9. Doi: 10.1109/TEC.2020.3020263. 30 July, 2021.
[3]. Maloma, E., Muteba, M. and Nicolae, D., (2017). Effect of Rotor bar Shape on the Performance of Three Phase Induction Motors with Broken Rotor Bars. 2017 international conference on optimization of electrical an electronic equipment (OPTIM). 364 – 369. Doi:10.1109/OPTIM.2017.7974997. 17 September, 2021.
[4]. Lipo, T. A. (2017). Introduction to AC Machine Design. New Jersey: IEEE Press, John Wiley & Sons, Inc. PP. 251 – 302.
[5]. Hughes, A., (2013). Electric Motors and Drives: Fundamentals, Types and Applications. 4th edition. Oxford: Newnes.
[6]. Williamson, S, & McClay, C. J. (1996). Optimization of the Geometry of Closed Rotor Slots for Cage Induction Motors. IEEE Transactions on Industry Applications, Vol. 32, No. 3,
[7]. Fireteanu, V. (2008). Squirrel-Cage Induction Motor with Intercalated Rotor Slots of Different Geometries. XIII International Symposium on Electromagnetic Fields in Mechatronics, Electrical and Electronic Engineering, September, 2007. DOI: 10.3233/978-1-58603-895-3-284.
[8]. Yeadon, W. H. and Yeadon, W. A. (2001). Handbook of Small Electric Motors. New York: The McGraw-Hill Companies, Inc. PP. 738 – 870.
[9]. Boldea, I. and Nasar, S. A. (2010). The Induction Machine Handbook. Washington, D.C: CRC Press, Taylor & Francis Group. PP. 447 – 473.
[10]. Say, M. G. (1978). Alternating Current Machines. Pitman Publishing Ltd. Fourth edition.
[11]. Vukosavic N. S. (2013). Electrical Machines. Springer New York Heidelberg Dordrecht London. ISBN: 978-1-4614-0400-2 (www.springer.com). DOI: 10.1007/978-1-4614-0400-2. Pp. 365 – 472.

[12]. Ibrahim, S. (2014). Centroid and Center of Mass of The Composite Bodies. https://www.researchgate.net/publication/307605237. DOI: 10.13140/RG.2.2.24991.36002.
[13]. Chapman, S. J. (2005). Electric Machinery Fundamentals. Fourth Edition. The McGraw-Hill Companies. Inc. ISBN 0-07-246523—9, www.mhhe.oom. Pp. 380 =472.
[14]. Pyrhonen, J., Jokinen, T. and Hrabovcova, V. (2014). Design of Rotating Electrical Machines. West Sussex: John Wiley & Sons, Ltd. PP. 293 – 388.
[15]. Gönen, T. (2012). Electrical Machines with Matlab. New York: Taylor & Francis Group, LLC. Pp. 207 – 262.
[16]. Cochran, P. L. (1989). Polyphase Induction Motors. Analysis Design and Application. Marcel and Dekker. NY. USA. ISBN 0-8247-8043-4. Pp. 427 – 585
[17]. Toliyat, H. A. and Kliman, G. B. (2004). Handbook of Electric Motors. Florida: Taylor & Francis Group. PP. 263 – 265.